# Toll-Like Receptors Are Part of the Innate Immune Defense System of Sponges (Demospongiae: Porifera)

*Matthias Wiens, Michael Korzhev, Sanja Perović-Ottstadt, Bérengère Luthringer, David Brandt, Stefanie Klein, and Werner E. G. Müller*

Institut für Physiologische Chemie, Abteilung Angewandte Molekularbiologie, Duesbergweg 6, Johannes Gutenberg Universität, D-55099 Mainz; Germany

During evolution and with the emergence of multicellular animals, the need arose to ward off foreign organisms that threaten the integrity of the animal body. Among many different receptors that participate in the recognition of microbial invaders, toll-like receptors (TLRs) play an essential role in mediating the innate immune response. After binding distinct microbial components, TLRs activate intracellular signaling cascades that result in an induced expression of diverse antimicrobial molecules. Because sponges (phylum Porifera) are filter feeders, they are abundantly exposed to microorganisms that represent a potential threat. Here, we describe the identification, cloning, and deduced protein sequence from 3 major elements of the poriferan innate response (to bacterial lipopeptides): the TLR, the IL-1 receptor–associated kinase-4–like protein (IRAK-4l), and a novel effector caspase from the demosponge *Suberites domuncula*. Each molecule shares significant sequence similarity with its homologues in higher Metazoa. Sequence homologies were found in particular within the family-specific domains toll/interleukin-1 receptor/resistance (TLR family), Ser/Thr/Tyr kinase domain (IRAK family), and CASc (caspase family). In addition, in situ hybridization and immunohistological analyses revealed an abundance of *SDTLR* (TLR) transcripts in epithelial layers of the sponge surface (exopinacoderm and endopinacoderm). Furthermore, it is shown that both *SDTLR* and *SDIRAK-4 like* (IRAK) are expressed constitutively, regardless of treatment with synthetic triacyl lipopeptide $Pam_3Cys\text{-}Ser\text{-}(Lys)_4$. In contrast, *SDCASL* (caspase) expression is highly $Pam_3Cys\text{-}Ser\text{-}(Lys)_4$ inducible. However, blocking of the lipopeptide with recombinant TLR prior to its application completely prevented the induced expression of this poriferan caspase. These results underscore that the phylogenetically oldest extant metazoan phylum is provided already with the signaling pathways of the antimicrobial host-defense system of Metazoa.

## Introduction

Innate immunity represents an efficient and complex first-line defense system that allows immediate response to microbial assaults. It is based on a set of germ cell–encoded receptors that are expressed at the surface of cells situated at host–environment boundaries. These evolutionary conserved molecules were termed pattern recognition receptors (PRRs) because in their function as sentinels of the innate immune system, they recognize highly conserved microbial structures that were termed pathogen-associated molecular patterns (PAMPs). PAMPs are essential for survival and pathogenesis of microorganisms, often representing a molecular signature characteristic of the pathogen class (Medzhitov and Janeway 2000). The recognition of such structures through PRRs reflects a strategy of the innate immune system to prevent the generation of escape mutants that would thus lack the ability to cause infection.

Toll-like receptors (TLRs) are among the best-characterized PRRs. By virtue of a conserved intracellular toll/interleukin-1 receptor/resistance (TIR) domain, they were grouped to the interleukin-1 (IL-1)/TLR superfamily, which also comprises receptors involved in inflammatory response, for example, cytokine receptor interleukin-1 receptor (IL-1R). However, toll receptors are further characterized by amino-terminal and extracellular leucine-rich repeats (LRRs; each 20–30 amino acids [aa] in length), whereas the IL-1Rs have extracellular immunoglobulin domains. Apart from the TLR and IL-1R subgroups, the TLR superfamily comprises a third subgroup, cytoplasmic adapter proteins with no extracellular region.

Key words: sponges, innate immunity, toll-like receptor, IRAK, TIR, death domain, caspase, lipoproteins.

E-mail: wiens@uni-mainz.de.

*Mol. Biol. Evol.* 24(3):792–804. 2007
doi:10.1093/molbev/msl208
Advance Access publication December 26, 2006



The toll protein was originally described as a type I transmembrane receptor that controls dorsoventral patterning of the *Drosophila* embryo (Hashimoto et al. 1988). In 1996, Lemaitre et al. demonstrated the involvement of the *Drosophila* toll receptor in the antifungal immunity. Since then, members of the ever increasing toll family have been identified in many other organisms, mostly through expressed sequence tag and genomic sequence database analyses. Thus, toll homologues were discovered in vertebrates, arthropods, and *Caenorhabditis elegans* (Medzhitov and Janeway 2000; Underhill and Ozinsky 2002; Akira 2003). PAMPs recognized by those TLRs include lipopolysaccharides (LPSs) and lipoproteins (LPs), peptidoglycans, flagellin, dsRNA, distinct nucleic acid motifs, etc. Upon direct or indirect ligation of PAMPs to TLRs the receptors homo- or heterodimerize, consequently triggering various conserved and intracellular signal cascades. In most cases this involves recruitment of cytoplasmic TIR domain–containing adapter molecules to the aggregated receptors, in particular MyD88, which also contains another protein interaction domain, the death domain (DD). Subsequently, MyD88 associates with the DD-bearing serine/threonine protein kinase IL-1 receptor–associated kinase-4 (IRAK-4) through homophilic DD–DD interaction, thus recruiting the kinase to the receptor–adapter complex. Following the activation of IRAK-4 downstream signaling leads to an activation of transcription factors, such as nuclear factor kappa B (NF-κB). Consequently, the expression of costimulatory and regulatory molecules is induced. Also, defense mechanisms that directly oppose foreign invaders are triggered, such as proapoptotic, proinflammatory, and immunomodulatory cytokines, antimicrobial peptides, or even proteolytic cascades that involve the key effectors of apoptotic cell death, the caspases (see: Takeda 2005). However, the reaction elicited often depends on the cell type; in human polymorphonuclear neutrophils, for example, TLR-induced activation of NF-κB

delayed apoptosis through modulation of Bcl-2 proteins (Francois et al. 2005).

Already since 1907, when Wilson (1907) documented the species-specific reaggregation of poriferan cells, sponges became a classical model for the study of cellular self/self- and self/nonself recognition. Because sponges are located near the root of the tree of metazoan life, they turned out to be highly suitable to study the molecular evolution of metazoan innate immunity. With the emergence of molecular biological techniques, a wealth of molecules involved in the poriferan innate immune response was identified. These findings are not surprising if one considers that sponges filter each day huge amounts of water through their aquiferous canal system in search of edible material. Because the aqueous milieu is rich in microorganisms (Bergh et al. 1989; Steward et al. 1996), the sessile sponges may easily suffer bacterial or fungal infections with lethal effect (Lauckner 1980; Vacelet et al. 1994). However, not only are Porifera a rich source of bioactive nonproteinaceous metabolites with potential antimicrobial function (Sarma et al. 1993; Proksch 1994; Faulkner 2002), but they are also provided with various proteinaceous molecules of defense that were honed to perfection during 800 MYR of evolution, ensuring the survival of the phylum. Among the poriferan proteins are those of apoptotic cell death (e.g., Bcl-2 and caspases [Wiens and Müller 2006]), antiviral defense (several 2′,5′-oligoadenylate synthetases [Wiens et al. 1999; Grebenjuk et al. 2002]), antifungal response (the 1(3)-β-D-glucan–binding protein [Perović-Ottstadt et al. 2004]), and antibacterial defense. The latter one features receptors of bacteria or bacterial products (Group A/B scavenger receptors [Blumbach et al. 1998; Pahler et al. 1998]), mediators (stress-activated mitogen-activated protein kinases p38 and c-jun N-terminal kinase [Böhm et al. 2000, 2001]), and effector molecules (lysozyme- and tachylectin-related molecules [Thakur et al. 2005]). Furthermore, the poriferan response to gram-negative bacteria was elucidated recently (Wiens et al. 2005). Thus, sponge LPS–interacting protein (SLIP), a transmembrane receptor on the sponge cell surface, was found to recognize and to bind the endotoxin LPS. After dimerization SLIP triggers intracellular signaling through interaction with poriferan MyD88 (myeloid differentiation factor 88), an adapter that bears 2 protein interaction domains, TIR and DD. Subsequently, signal transduction analysis showed that exposure of sponge cells to LPS resulted in an elevated expression of MyD88 and of macrophage expressed gene, a perforin-like executing molecule with antibacterial (gram-negative) effect.

Sponges are filter feeders and thus highly exposed to bacterial invaders. Because LPs are nearly ubiquitous constituents of bacterial cell walls, sponges were screened for the molecular repertoire that is part of the LP-stimulated innate immune response. In the present study, we report on the identification of a TLR, a serine/threonine protein kinase (IRAK-4l), and a novel effector caspase in the sponge *Suberites domuncula*. To underscore the function of these molecules in the antimicrobial defense system, *S. domuncula* was exposed to $Pam_3Cys\text{-}Ser\text{-}(Lys)_4$, a synthetic triacyl lipopeptide that mimics bacterial LPs. In response to this lipopeptide challenge, TLR and IRAK-4l displayed a constitutive expression. In contrast, the expression of the poriferan effector caspase dramatically increased. This effect could be blocked in competition experiments with recombinant TLR (rTLR). Furthermore, in situ hybridization studies revealed a predominant expression of TLR in the cell layer of the sponge surface and also in cells lining the aquiferous canal system.

## Materials and Methods

### Chemicals and Enzymes

The sources of chemicals and enzymes used were given previously (Wiens et al. 2005). In addition, (S)-[2,3-bis(palmitoyloxy)-(2-RS)-propyl]-N-palmitoyl-(R)-Cys-(S)-Ser-(S)-$Lys_4$-OH·3HCl ($Pam_3Cys\text{-}Ser\text{-}(Lys)_4$) was purchased from Axxora Deutschland GmbH (Grünberg, Germany); natural sterile-filtered seawater (SW) was obtained from Sigma-Aldrich (Taufkirchen, Germany); PCR-DIG-Probe Synthesis Kit, CDP-Star (disodium 2-chloro-5-(4-methoxyspiro{1,2-dioxetane-3,2′-(5′-chloro)-tricyclo [3.3.1.1.3,7]decan}-4-yl)phenyl phosphate), 4-nitro blue tetrazolium chloride (NBT), 5-bromo-4-chloro-3-indolyl phosphate (BCIP), and anti-DIG Fab fragments conjugated to alkaline phosphatase (anti-DIG-AP) from Roche Applied Science (Mannheim, Germany); TRIzol Reagent, SNAP Total RNA Extraction Kit, and competent TOP10 cells from Invitrogen (Karlsruhe, Germany); and Hybond $N^+$ and antihistidine antibody from GE Healthcare Europe GmbH (Munich, Germany).

### Sponges

Specimens of the marine sponge *S. domuncula* (Porifera, Demospongiae, Hadromerida) were collected near Rovinj (Croatia) in the northern Adriatic Sea and then kept in aquaria in Mainz (Germany) at 17 °C.

### Cloning of the Poriferan TLR *SDTLR*, the IRAK-4l Protein *SDIRAK4l*, and the Caspase-Like Protease *SDCASL*

The complete sponge cDNA *SDTLR*, coding for the putative poriferan TLR_SUBDO, was isolated from a *S. domuncula* cDNA library (Kruse et al. 1997). A degenerate forward primer, 5′-AAA/G ATT/C/A GTI A/GTI GTI G/C/TTI A/TG/C-3′ (where I = inosine), was designed against a stretch of conserved aa, K-I-V-I/V-V-L/V-S, that is part of the TIR domain (Smart accession number SM00255). In combination with a library-specific primer, polymerase chain reaction (PCR) was carried out at an initial denaturation for 5 min at 95 °C, followed by 35 amplification cycles at 95 °C for 30 s, 54 °C for 45 s, and 74 °C for 1 min, and terminated with a final extension at 74 °C for 10 min. Thus, a fragment of ≈400 bp was isolated and subsequently sequenced by means of an automatic DNA sequenator (Li-Cor 4200). Ultimately, the *SDTLR* sequence was completed through primer walking.

Likewise, the complete poriferan cDNAs *SDIRAK-4l* and *SDCASL* were isolated from the *S. domuncula* cDNA library: application of the degenerate forward primer 5′-CAT/C C/AGI GAT/C A/GTI AAA/G T/AC/GI GCI AA-3′ (directed against the IRAK-4 catalytic site H-R-D-I/V-K-S-A-N [Prosite Pattern accession number PS00108]) and the degenerate forward primer 5′-T/CTI

ATT/C/A CAA/G GCI TGT/C A/T/CG/TI GG-3′ (directed against the caspase Cys active site L/F-I-D-A-C-R/L-G [accession number PS01122]) resulted in fragments of ≈700 bp and ≈1200 bp, respectively. Again, the fragments were completed by using a combination of sequence-specific and library-specific primers.

### Sequence Analyses

Via the servers at the European Bioinformatics Institute, Hinxton, United Kingdom (http://www.ncbi.nlm.nih.gov/BLAST/) and the National Center for Biotechnology Information (NCBI), Bethesda, MD (http://www.ncbi.nlm.nih.gov/BLAST/) homology searches were performed. Multiple alignments were carried out with ClustalW version 1.6 (Thompson et al. 1994). Phylogenetic trees were constructed on the basis of aa sequence alignments applying the Neighbor-Joining method to the distance matrices that were calculated using the Dayhoff PAM matrix model (Dayhoff et al. 1978; Saitou and Nei 1987). The degree of support for internal branches was further assessed by bootstrapping (Felsenstein 1993). The graphical output of the bootstrap figures was produced through the "Treeview" software (R. D. M. Page, University of Glasgow, United Kingdom; http://taxonomy.zoology.gla.ac.uk/rod/treeview.html). Further graphic presentations were prepared with GeneDoc (Nicholas KB and Nicholas NB 1997). Potential subunits, domains, patterns, and transmembrane regions were predicted after searching the Pfam database (Finn et al. 2006; http://www.sanger.ac.uk/Software/Pfam/), the SMART database (Letunic et al. 2006; http://smart.embl-heidelberg.de/), or according to Kyte and Doolittle (1982).

### Preparation of Recombinant TLR_SUBDO

The forward primer 5′-GGATCCACATGTCCACCTTTTCTT-3′ (*Bam*HI site is underlined) and the reverse primer 5′-GTCGACTACACTCTAACCAGACCAC-3′ (*Sal*I site is underlined) were used to amplify the complete open reading frame (ORF) of *SDTLR* ($nt_{132–1011}$), including $Met_{start}$ and stop codon. This cDNA was ligated in frame into the bacterial expression vector pQE32 (Qiagen, Hilden, Germany). The rTLR protein, tagged with an amino-terminal, 6× His stretch, was expressed in TOP10 *Escherichia coli* cells, extracted with BugBuster Protein Extraction Reagent (Novagen, Madison, WI), and purified through nickel-nitrilotriacetic acid (Qiagen) resin treatment (Hochuli et al. 1987). Protein concentrations were determined according to Lowry et al. (1951). Subsequently, the protein was checked by 12% polyacrylamide gels containing 0.05% sodium dodecyl sulfate (Laemmli 1970). Ultimately, after blotting on polyvinylidene fluoride membranes (Millipore, Billerica, MA), the recombinant protein was detected with antihistidine antibodies.

### Incubation of Sponge Tissue with $Pam_3Cys$-Ser-$(Lys)_4$

*Suberites domuncula* tissue samples were exposed to the synthetic lipopeptide (S)-[2,3-Bis(palmitoyloxy)-(2-RS)-propyl]-N-palmitoyl-(R)-Cys-(S)-Ser-(S)-$Lys_4$-OH·3HCl ($Pam_3Cys$-Ser-$(Lys)_4$) in SW at a final concentration of 60 μg/ml for up to 32 h. In another series of experiments, $Pam_3Cys$-Ser-$(Lys)_4$ was preincubated for 30 min with recombinant *S. domuncula* TLR (rTLR; 6 mg/ml), prior to the exposition of sponge tissue.

### In Situ Localization Studies

The in situ hybridization method applied is based on a procedure described by Polak and McGee (1998) with modifications recently described (Perović et al. 2003). In short, frozen sections (8 μm) of sponge tissue samples (control or $Pam_3Cys$-Ser-$(Lys)_4$ treated) were fixed in 4% paraformaldehyde, then incubated with proteinase K (1 μg/ml), and fixed again in paraformaldehyde. Hybridization was performed overnight at 45 °C in 2 × SSC sodium chloride/sodium citrate (SSC supplemented with 50% formamide), either with sense (control) or antisense probes. The single-stranded DNA probes (230 nt in size) had been labeled with the PCR-DIG-Probe Synthesis Kit through PCR using a part of the TIR domain of *SDTLR* as linearized template. Following hybridization the sections were washed at 50 °C at decreasing salt concentrations (1 × SSC to 0.2 × SSC), blocked, and then incubated with anti-DIG Fab fragments, conjugated to alkaline phosphatase. Through addition of NBT and BCIP, hybridized probes were visualized.

### RNA Extraction and Northern Blotting Analyses

Total RNA was isolated through lysis of homogenized and pulverized tissue (control, $Pam_3Cys$-Ser-$(Lys)_4$–, or $Pam_3Cys$-Ser-$(Lys)_4$/rTLR–treated *S. domuncula* tissue), using TRIzol Reagent as described earlier (Grebenjuk et al. 2002). Following purification with SNAP Total RNA Isolation Kit, 5 μg of total RNA each was size separated and blotted on Hybond $N^+$ membrane. Hybridization was performed with a *SDTLR* probe ($nt_{607–1008}$, encoding the TIR domain), *SDIRAK-4l* probe ($nt_{199–1070}$, encoding most of the STYKc domain), or *SDCASL* probe ($nt_{49–822}$, encoding the putative p20 and p10 subunits). Furthermore, a probe was designed to detect the expression of the housekeeping gene β-tubulin (TUB) (*SDTUB*, $nt_{83–483}$; accession number AJ550806) as reference. Prior to the hybridization the probes had been labeled with DIG-11-deoxyuridine triphosphate through the PCR-DIG-Probe Synthesis Kit (according to the manufacturer's instructions). Hybridized probes were detected with anti-DIG Fab fragments (conjugated to alkaline phosphatase) and visualized by the chemiluminescence technique using cytidine 5′ diphosphate (CDP) Star as substrate.

### Antibody Preparation and Immunohistological Analysis

Polyclonal antibodies (pAbs) were raised against recombinant TLR_SUBDO in female rabbits (White New Zealand) as described (Harlow and Lane 1988; Wimmer et al. 1999). In control experiments, 100 μl of the pAbs were adsorbed to 20 μg of the recombinant protein during an incubation period of 30 min (4 °C) prior to their use. Sponge tissue was fixed in paraformaldehyde, embedded in Technovit 8100 (Heraeus Kulzer, Wehrheim, Germany), and sectioned, as described (Grebenjuk et al. 2002). Sections of 2 μm were then incubated first with pAbs (1:1000 dilution) and subsequently with Cy3-conjugated goat anti-rabbit IgG (Sigma-Aldrich). The sections were

inspected for immunofluorescence with an Olympus AHBT3 microscope. Control experiments with preimmuneserum did not show autoimmunofluorescence.

## Results and Discussion

### Cloning of the Poriferan Toll-Like Receptor *SDTLR*

The complete *SDTLR* cDNA was isolated from a *S. domuncula* cDNA library by means of PCR and a degenerate primer that was directed against a conserved region within the TIR domain of TLRs. *SDTLR* consists of 1,274 nt (excluding the poly(A) tail) that embrace an ORF of 1,008 nt (excluding the first stop codon), beginning at $nt_{134–137}$ ($Met_{start}$). During northern blot analyses, a DIG-labeled *SDTLR* probe detected a transcript whose size was consistent with that of the cDNA (≈1,300 nt; fig. 4). The deduced protein was termed TLR_SUBDO and contains 336 aa with an expected size of 37750 D. TLR_SUBDO shows significant sequence similarity to TLR-1 of *Gallus gallus* with an expect value (*E* value; Coligan et al. 2000) of $6 \times 10^{-7}$, but also to human/murine TLR-6 (*E* value = $3 \times 10^{-6}/5 \times 10^{-6}$) or human/murine TLR-1 (*E* value = $5 \times 10^{-6}$, both).

TLRs are characterized by a COOH-terminal intracellular TIR domain, required for the interaction with adapter proteins that equally contain a TIR domain. Furthermore, TLRs bear a transmembrane region as well as several LRRs (2–42 motifs of 20–30 aa in length) in their amino-terminal extracellular part.

Bell et al. (2003) devised a consensus sequence for LRRs of higher Metazoa. Accordingly, LRRs consist of a leucine-bearing portion (consensus: x-L-x(2)-L-x-L-x(2)) required for binding of PAMPs and a helical portion (HP) (consensus: [SNTC]-x-Ø-x(2)-Ø-x(4)-F-x(2)-L; Ø = any hydrophobic residue). However, deviation from these patterns both in length and in sequence is not uncommon among TLRs.

TLR_SUBDO displays 2 of those major characteristics of the TLR superfamily: a TIR domain ($aa_{198–333}$, *E* value = $5.4 \times 10^{-6}$; Smart accession number SM00255) and a transmembrane anchor ($aa_{44–66}$; Kyte and Doolittle 1982). Yet, no LRRs sensu stricto were identified in TLR_SUBDO and the putative extracellular amino terminus (eN-t) is unusually short (43 aa). However, the eN-t of the poriferan TLR has an elevated occurrence of polar or charged aa (65%) and does contain a number of leucine residues as well as valine and serine residues (total of 16). Interestingly, the arrangement of aa revealed a pattern, with [FV]-x(1,2)-[SN]-L 4 times repeated (fig. 1*A*). The number of these repeats is smaller than in TLRs of higher Metazoa and the repeats follow only marginally the consensus pattern of the ligand-binding portion. Nevertheless, after the last repeat the poriferan TLR sequence completely fits the consensus of the HP (fig. 1*A*).

### Phylogenetic Analysis of the Poriferan TLR

The toll receptor was initially identified as a protein that is essential for the dorsoventral polarity during *Drosophila* embryogenesis. Since then, further homologues of the toll receptor (bearing the characteristic TIR domain) have been found not only in *Drosophila* and other insects but also in vertebrates (at least 10 human TLRs have been characterized, several more in other vertebrates) and in the nematode *C. elegans*.

Furthermore, TIR domains were also found in several adapter proteins (e.g., MyD88, TRIF [TIR-domain-containing adaptor inducing interferon-beta], and TIRAP [TRIF-related adaptor molecule]) that regulate downstream signaling upon activation of TLRs. In addition, several toll-related proteins that contain TIR have been discovered in plants, where they are implicated in the resistance to pathogens (Jebanathirajah et al. 2002). However, little evidence exists that this limited structural similarity reflects evolutionary conservation of an ancient signaling pathway. There are not only no similarities in downstream signaling pathways activated by metazoan TLR and plant disease resistance proteins, but there is also in general no overlap between immune signaling components of plants and animals (Ausubel 2005).

Interestingly, sequence analyses of the poriferan putative TLR displayed higher aa sequence similarity to vertebrate TLRs than to those of invertebrates, especially regarding the protein interaction domain TIR (fig. 1*B*). Thus, TLR_SUBDO shares 21% identical and 37% similar aa of its TIR with the respective domain of human TLR-1 and chicken TLR-6, 20%/38% with TIR of human TLR-10, and 22%/36% with the murine TLR-6 TIR domain.

To determine the phylogenetic relationship of the poriferan TLR, molecular phylogenetic analyses were performed by the Neighbor-Joining method (Saitou and Nei 1987). Based on the significant similarities between the poriferan protein and TLRs, the TIR domain of TLR_SUBDO was aligned with the corresponding domain of representative members of the metazoan taxa, also including the only other known poriferan TIR domain of the recently discovered MyD88_SUBDO (Wiens et al. 2005). After rooting with the TIR domain of the plant *Medicago truncatula* TIR/disease resistance protein, the resulting phylogenetic tree revealed 2 clusters (fig. 1*C*). The first one contains insect TLRs, whereas the second one exclusively comprises vertebrate sequences. The latter one is further divided into 5 groups, containing TLR-2, TLR-3/5, TRL-4, TLR-7/8/9, and TLR-1/6/10. The poriferan TLR appears near the root of the phylogenetic tree, at the origin of the aforementioned clusters, closely followed by MyD88_SUBDO. However, the phylogenetic relationship of the *C. elegans* TIR domain protein family member could not be resolved.

These phylogenetic analyses revealed that the poriferan TLR shares a common ancestor with the TLRs of invertebrates and vertebrates, as indicated by robust bootstrap values. In the course of evolution the ancestral gene likely duplicated several times leading to a family of proteins that has at least 10 members in humans. Because the extracellular LRR domains of TLRs are implicated in recognition and binding of PAMPs (Bell et al. 2003), their subsequent evolutionary diversification probably allowed an enhanced distinction between a vast array of structurally unrelated microbial ligands in higher Metazoa.

### Cloning of the Poriferan IRAK-4l Protein *SDIRAK-4l*

*SDIRAK-4l* was isolated from a *Suberites* cDNA library by means of a degenerate primer, designed to target

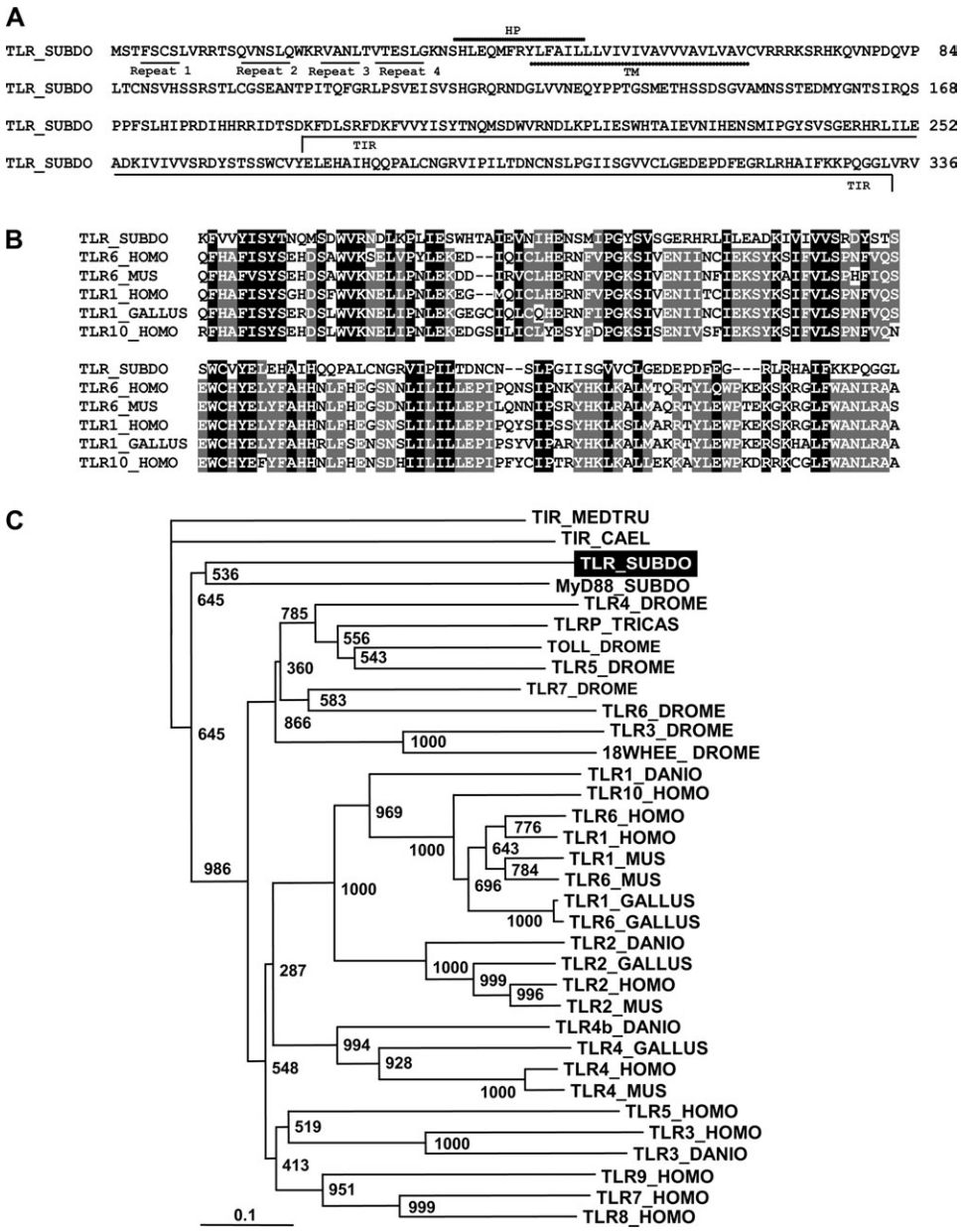


FIG. 1.—*Suberites domuncula* TLR. (*A*) The deduced poriferan TLR aa sequence of *S. domuncula* (TLR_SUBDO) is depicted. Four extracellular repeats of a leucine-containing motif are shown as well as the HP, the putative transmembrane stretch, and the intracellular TIR domain. (*B*) The TIR domain of TLR_SUBDO ($aa_{198–333}$) was aligned with the respective domain of human TLR-10 (TLR10_HOMO; NCBI accession number AAI09113; $aa_{633–774}$), TLR-6 (TLR6_HOMO; BAA78631; $aa_{641–780}$), and TLR-1 (TLR1_HOMO; NP_003254; $aa_{636–775}$), *G. gallus* TLR-1 (TLR1_GALLUS; NP_001007489; $aa_{647–788}$), and murine TLR-6 (TLR6_MUS; AAH55366; $aa_{641–779}$). Residues conserved (identical or similar with respect to their physicochemical properties) in all sequences are shown in white letters on black; those in 80% are in white letters on gray. (*C*) Rooted tree generated after alignment of the aforementioned TIR domains, further integrating the TIR domains of human TLR-9 (TLR9_HOMO; NP_059138; $aa_{870–974}$), TLR-8 (TLR8_HOMO; NP_057694; $aa_{898–1040}$), TLR-7 (TLR7_HOMO; NP_057646; $aa_{890–1035}$), TLR-5 (TLR5_HOMO; AAC34376; $aa_{692–827}$), TLR-4 (TLR4_HOMO; CAH72620; $aa_{474–615}$), TLR-3 (TLR3_HOMO; AAH94737; $aa_{755–899}$), and TLR-2 (TLR2_HOMO; AAH33756; $aa_{640–784}$), of *Drosophila melanogaster* TOLL (TOLL_DROME; NP_733166; $aa_{858–995}$), TOLL-7; (TLR7_DROME; AAF86225; $aa_{1098–1235}$), TOLL-6 (TLR6_DROME; AAF86226; $aa_{1114–1245}$), TOLL-5 (TLR5_DROME; AAF86227; $aa_{643–779}$), TOLL-4 (TLR4_DROME; AAF86228; $aa_{658–794}$), TLR-3 (TLR3_DROME; AAF86229; $aa_{645–781}$), and 18 wheeler (18WHEEL_DROME; NP_476814; $aa_{1045–1182}$), of *Caenorhabditis elegans* TIR domain protein family member (TIR_CAEL; NP_497785; $aa_{366–506}$), of *G. gallus* predicted TLR-6 (TLR6_GALLUS; XP_428184; $aa_{275–413}$), TLR-4 (TLR4_GALLUS; NP_001025864; $aa_{688–825}$), TLR-2 (TLR2_GALLUS; NP_989609; $aa_{649–793}$), of *D. rerio* TLR4b (TLR4b_DANIO; NP_997978; $aa_{673–814}$), TLR-3 (TLR3_DANIO; AAQ91307; $aa_{34–176}$), TLR-2 (TLR2_DANIO; NP_997977; $aa_{641–784}$), TLR-1 (TLR1_DANIO; XP_697531; $aa_{619–761}$), of *Tribolium castaneum* predicted protein similar toll protein precursor (TLRP_TRICAS; XP_967796; $aa_{837–972}$), of murine TLR-4 (TLR4_MUS; AAH29856; $aa_{672–813}$), TLR-2 (TLR2_MUS; NP_036035; $aa_{640–784}$), TLR-1 (TLR1_MUS; NP_109607; $aa_{639–779}$), of *S. domuncula* MyD88 (MyD88_SUBDO; CAI68016; $aa_{114–251}$), and of the plant *Medicago truncatula* TIR/disease resistance protein (TIR_MEDTRU; ABE93165; $aa_{24–162}$). The latter one was used as an outgroup. The scale bar indicates an evolutionary distance of 0.1 aa substitutions per position in the sequence. The numbers at the nodes are an indication of the level of confidence for branching (1,000 bootstrap replicates).

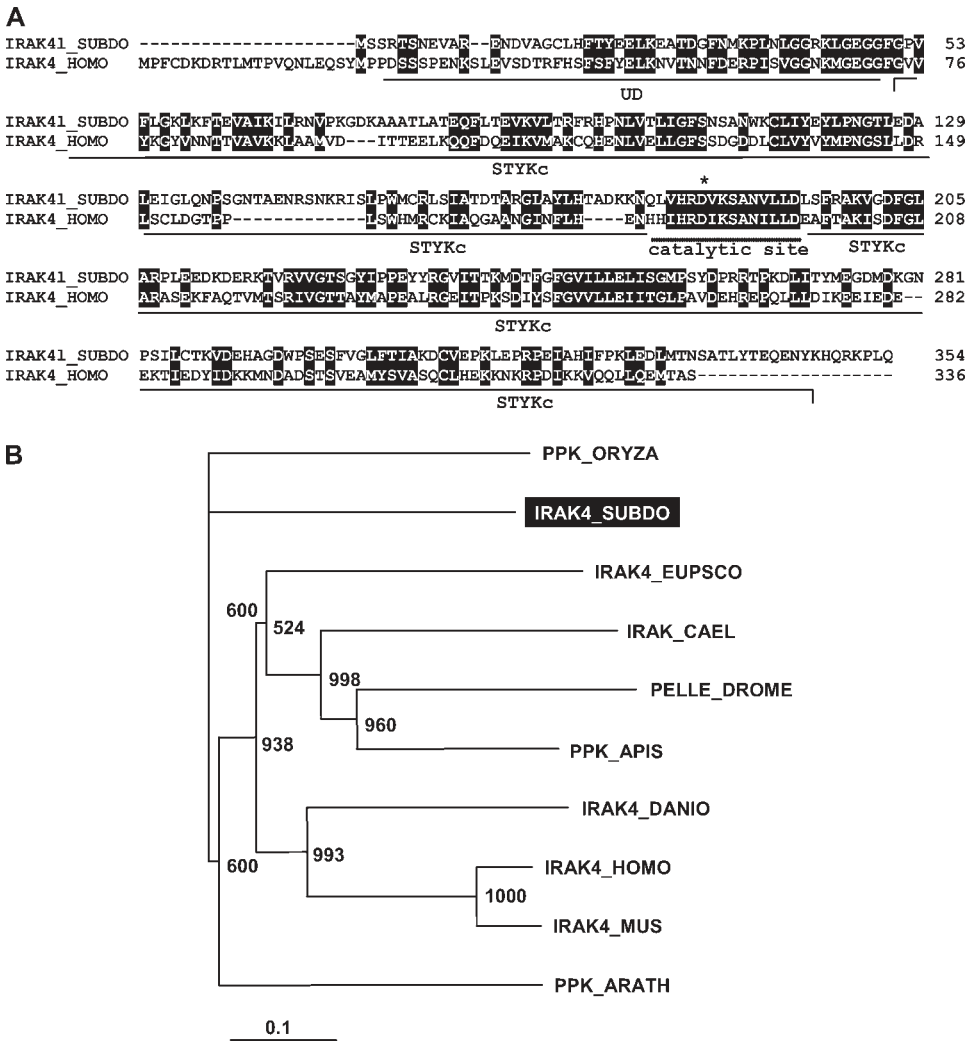


FIG. 2.—*Suberites domuncula* IRAK-4l. (*A*) The deduced poriferan IRAK-4l sequence (IRAK4l_SUBDO) was aligned with the human IRAK-4 short-form variant 4 (IRAK4_HOMO; AAR02363). The characteristic STYKc domain, the catalytic site, the critical aspartate residue (asterisk), and the undetermined region (UD) are marked. (*B*) Rooted tree constructed after alignment of the STYKc domains present in the IL-1 receptor–associated kinase of *Euprymna scolopes* (IRAK4_EUPSCO; AAY27972; $aa_{258–521}$), Pelle CG5974-PA of *Drosophila melanogaster* (Pelle_DROME; NP_476971; $aa_{185–474}$), Pelle IRAK-like kinase-1 of *Caenorhabditis elegans* (IRAK_CAEL; AAK37545; $aa_{185–474}$), predicted protein kinase of *Apis mellifera* (PPK_APIS; XP_624002; $aa_{155–373}$), human IRAK-4 short-form variant 4 (IRAK4_HOMO; AAR02363; $aa_{65–328}$), IRAK-4 of *D. rerio* (IRAK4_DANIO; AAT37635; $aa_{218–483}$), murine IRAK-4 (IRAK4_MUS; NP_084202; $aa_{189–459}$), IRAK-4l protein of *S. domuncula* (IRAK4l_SUBDO; $aa_{52–346}$), putative protein kinase of *Arabidopsis thaliana* (PPK_ARATH; AAF99862; $aa_{290–567}$), and putative receptor protein kinase of *Oryza sativa* (PPK_ORYZA; XP_550056; $aa_{345–618}$) that was used as an outgroup.

the catalytic site of Ser/Thr/Tyr kinase domain (STYKc domain, Smart accession number SM00221) that generally characterizes IRAKs. The complete cDNA comprises 1,254 nt (excluding the poly(A) tail) that contain an ORF of 1,062 nt ($nt_{40–42}$ [$Met_{start}$] to $nt_{1102–1104}$ [Stop]), encoding a putative protein of 354 aa (expected molecular weight [$M_r$] of 39,619) that was termed IRAK4l_SUBDO. Northern blot analyses confirmed the size of the transcript (fig. 4*A*).

IRAK4l_SUBDO displays highest sequence similarity to the human short form of IRAK-4 ($E$ value $= 2 \times 10^{-43}$), to murine IRAK-4 ($2 \times 10^{-41}$), and to *Danio rerio* IRAK-4 ($1 \times 10^{-37}$). Within the IRAK-4l sequence homology searches revealed the STYKc domain at $aa_{90–384}$ ($E$ value $= 3.1 \times 10^{-20}$) with the putative catalytic site at $aa_{218–230}$ (fig. 2*A*) that follows the established Prosite Pattern without exception (accession number PS00108). Intriguingly, no DD motif could be identified in the amino-terminal part of IRAK-4l, which appears to be truncated, possibly the result of alternative splicing (see below). However, a probe targeting the STYKc domain of IRAK-4l revealed only one band of the expected size.

## Phylogenetic Analysis of the Poriferan IRAK-4l Protein

IRAKs constitute a family of serine/threonine kinases, originally identified through coprecipitation of activated IL-1 receptor (Martin et al. 1994). The mammalian IRAK family consists of at least 4 members that mediate the activation of transcription factors (especially NF-κB) and mitogen-activated protein kinases: IRAK-1, IRAK-2, IRAK-4, and

IRAK-M, with different splice variants that are sometimes highly truncated. However, only IRAK-1, IRAK-4, and Pelle (*Drosophila melanogaster* IRAK homologue) contain a functional catalytic site within the kinase domain STYKc, with a critical aspartate residue ($D_{187}$ for human IRAK-4 short-form variant 4). In IRAK-2 and IRAK-M, this critical residue has changed into a serine or an asparagine, rendering their kinase domain inactive (Wesche et al. 1999). Furthermore, IRAK-1, IRAK-2, and IRAK-M but not Pelle or IRAK-4 contain a COOH-terminal region required for interaction with downstream adapter molecules. The recently identified IRAK-4 appears to be the apical kinase in the TLR-signaling pathways (Li et al. 2002). So far, only a limited number of IRAK-4 homologues have been identified in vertebrates and others in insects (*D. melanogaster* [Pelle] and *Apis mellifera* [predicted protein kinase]), nematodes (*C. elegans* [Pelle IRAK-like kinase]), and gastropods (*Euprymna scolopes* [IRAK]). Again, the poriferan protein shows highest sequence homology to vertebrate proteins, in particular to human IRAK-4 (27% identical and 40% similar aa) and to the murine protein (21%/32%). Also, it comprises the characteristic STYKc domain, with the critical aspartate residue ($D_{184}$) suggesting an active kinase.

On the other hand, IRAK4l_SUBDO does not include the amino-terminal DD that is required for homophilic DD–DD interaction with the upstream adapter MyD88. At least one mammalian variant of IRAK-4 (IRAK-4 short-form variant 4; AAR02363) also misses DD, indicating the conservation of this truncated version. How IRAK4l_SUBDO or IRAK-4 short-form variant 4 are recruited to upstream adapter molecules and thus to the TLRs is currently unknown. The amino-terminal stretch (UD for undetermined region; fig. 2*A*) that precedes the STYKc domain might be involved in recruitment to adapter proteins that either mediate MyD88-independent signal transduction or facilitate the binding to MyD88.

Because the poriferan IRAK-4l protein is characterized by a truncated amino-terminal part, only the conserved STYKc domain was considered for phylogenetic studies. Given that no plant IRAKs are known, the resulting tree was rooted with STYKc of the distantly related putative serine/threonine protein kinase of *Oryza sativa*. Thus, 2 clusters were revealed, containing either invertebrate IRAK-4 molecules or their vertebrate homologues. However, the latter one also features a mollusk protein at its basis. Nevertheless, the poriferan IRAK-4l protein appears at the origin of both clusters, hence forming the basis of the IRAK-4 family (fig. 2*B*).

## Cloning of the Poriferan Caspase–Like Protease *SDCASL*

Caspases (cysteine-dependant aspartyl-specific proteases) are highly selective cysteine proteases that cleave their substrate after an aspartic acid residue that is part of a tetrapeptide motif, hence leading to the dismantlement of the apoptotic cell (Takahashi and Earnshaw 1996; Thornberry and Lazebnik 1998).

After identification of *SDCASL* through degenerate primer PCR, targeting the cysteine catalytic site, a complete clone (1,681 nt, excluding poly(A)) was isolated from the *Suberites* cDNA library. Subsequently, the correct size of the *SDCASL* transcript was verified on northern blot (fig. 4*A*). *SDCASL* comprises an ORF between $nt_{148–150}$ ($Met_{start}$) and $nt_{1579–1581}$ (Stop), coding for a putative protein of 477 aa that was termed CASL_SUBDO (expected $M_r$ of 53475). This protein revealed greatest sequence homologies to caspase-7, especially to human caspase-7 chain A/B (*E* value = $2 \times 10^{-11}$), but also to *Drosophila* DCP-1 ($7 \times 10^{-11}$) and to caspase-8 of *Bos taurus* ($5 \times 10^{-9}$).

Different caspases have different domain architecture depending on their role in the apoptotic process (Salvesen and Dixit 1997; Thornberry et al. 1997). However, all of them are expressed as zymogens containing the CASc domain (Smart00115). In order to become active as cysteine peptidases, this domain has to be cleaved into a large (p20) and a small (p10) subunit. CASL_SUBDO putatively represents such a proenzyme comprising the 2 subunits, p20 ($aa_{17–152}$) and p10 ($aa_{184–274}$) (fig. 3*A*). As a general rule, p20 harbors the catalytic cysteine, histidine, and glycine residues that are part of conserved patterns. Regarding the caspase family-specific cysteine active site CASL_SUBDO follows the established pattern [K**M**]-P-K-[LIVMF]-[LIVMFY]-[LIVMF](2)-[QP**D**]-[AF]-C-[RQG**L**]-[GE] (Prosite Pattern PS01122) with 3 exceptions (marked in bold). However, the sequence homologous to the histidine active site (PS01121) revealed a surprising number of alterations (marked in bold): [H**P**]-x(2,4)-[SC]-x(2)-{A}-x(**0**,1)-[LIVMF**Y**](2)-[ST]-**G**-H-G. Thus, CASL_SUBDO bears the cysteine, histidine, and glycine residues that form the catalytic triad. Yet, it also features variations of otherwise conserved positions. This change might impose a novel substrate cleavage specificity for this poriferan caspase. Furthermore, similar to caspase-7 of other species and downstream caspases in general, the *Suberites* caspase-like protease only has a small amino-terminal prodomain ($aa_{1–16}$) and does not carry the large prodomain that is characteristic of initiator caspases (see below). Consequently, CASL belongs to the group of downstream caspases. These effector caspases usually cleave key regulatory and structural proteins with a preference of a D/VEXD sequence at the cleavage site of their substrates (Srinivasula et al. 1996; Talanian et al. 1997; Thornberry et al. 1997). However, CASL carries an uncharacteristically large COOH-terminal stretch of 203 aa following the p10 subunit. This segment ($aa_{275–477}$) revealed no similarity to any published sequence so far except a weak homology (*E* value = $7.5 \times 10^{-2}$) to a double stranded RNA–binding motif ($aa_{405–475}$; Pfam accession number PF0035.11).

## Phylogenetic Analysis of the Poriferan Caspase–Like Protein

The identification of CED-3, a *C. elegans* homologue to human mammalian caspase-1, provided the first evidence that the apoptotic cell death machinery is conserved across species (Yuan et al. 1993). Currently, 13 members of the caspase family have been identified in humans alone; at least 3 caspases were predicted to be present in the proteome of the sea urchin *Strongylocentrotus purpuratus*, and not less than 6 caspases were found in *D. melanaogaster*, 4 in *C. elegans*, and 4 in sponges (including *SDCASL*).

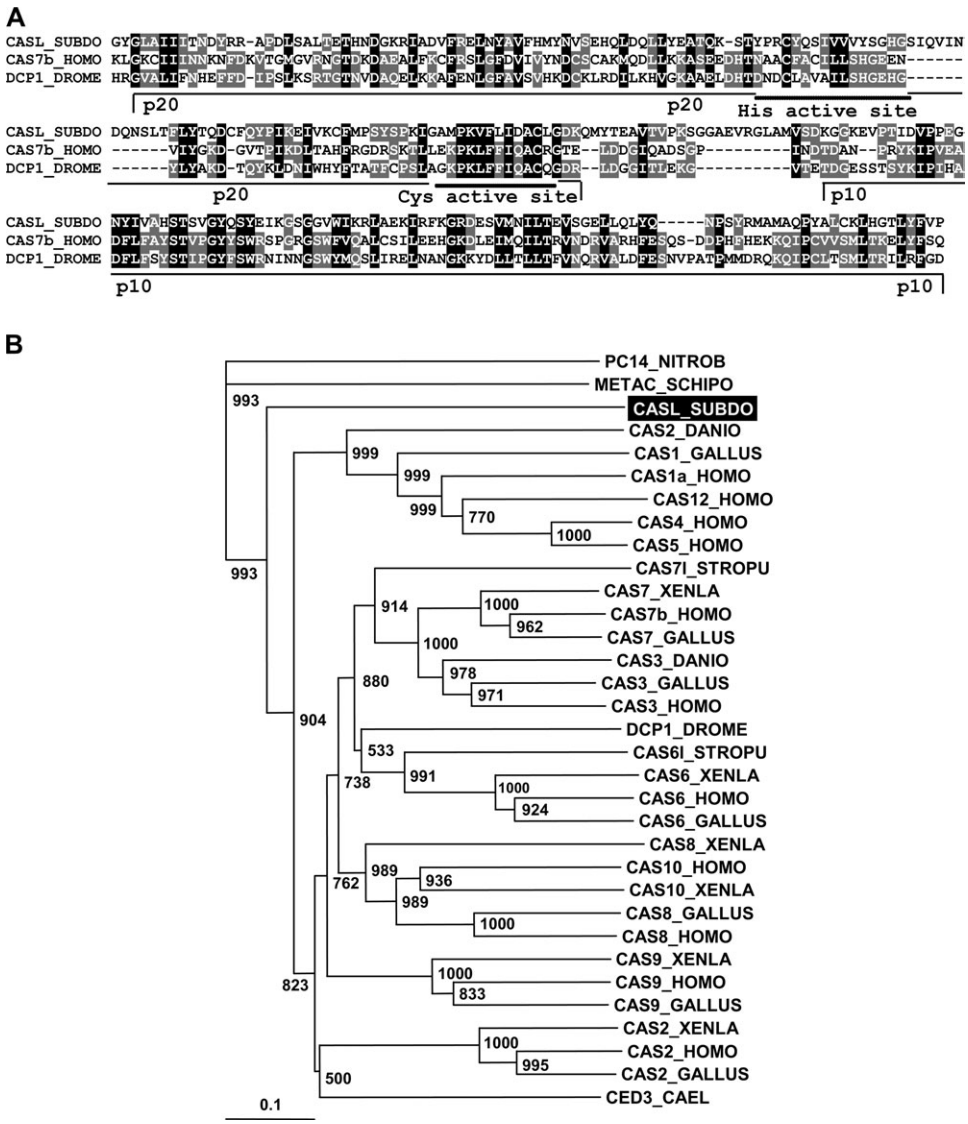


FIG. 3.—*Suberites domuncula* CASPL. (*A*) The CASc domain of the deduced poriferan caspase–like sequence (CASL_SUBDO; $aa_{17–247}$) was aligned with that of human caspase-7 chain B (CAS7b_HOMO; 52695494; $aa_{68–305}$) and of *Drosophila melanogaster* caspase DCP-1 (DCP1_DROME; AAB58237; $aa_{77–315}$). The putative subunits contained within (p20 and p10) are marked as well as the Cys and His active sites. (*B*) Rooted tree generated after alignment of CASc domains of human caspases: caspase-12 (CAS12_HOMO; AAQ88589; $aa_{103–338}$), caspase-10 (CAS10_HOMO; NP_001221; $aa_{232–471}$), caspase-9 (CAS9_HOMO; AAC50640; $aa_{152–414}$), caspase-8 (CAS8_HOMO; NP_001219; $aa_{242–494}$), caspase-7 chain B, caspase-6 (CAS6_HOMO; NP_001217; $aa_{37–289}$), caspase-5 (CAS5_HOMO; NP_004338; $aa_{166–415}$), caspase-4 (CAS4_HOMO; NP_150649; $aa_{69–318}$), caspase-3 (CAS3_HOMO; AAA65015; $aa_{37–275}$), caspase-2 (CAS2_HOMO; AAH02427; $aa_{191–446}$), and caspase-1a (CAS1a_HOMO; NP_150634; $aa_{152–401}$); *Xenopus laevis* caspases: caspase-10 (CAS10_XENLA; AAS91709; $aa_{260–496}$), caspase-9 (CAS9_XENLA; BAA94750; $aa_{136–397}$), caspase-8 (CAS8_XENLA; BAA94749; $aa_{252–495}$), caspase-7 (CAS7_XENLA; BAA94748; $aa_{71–316}$), caspase-6 (CAS6_XENLA; BAA94747; $aa_{50–299}$), and caspase-2 (CAS2_XENLA; BAA94746; $aa_{160–413}$); *D. rerio* caspases: caspase-3 (CAS3_DANIO; NP_571952; $aa_{39–280}$) and caspase-2 (CAS2_DANIO; AAG45230; $aa_{163–401}$); *G. gallus* caspases: caspase-9 (CAS9_GALLUS; AAL23701; $aa_{143–400}$), caspase-8 (CAS8_GALLUS; NP_989923; $aa_{228–480}$), caspase-7 (CAS7_GALLUS; XP_421764; $aa_{216–460}$), caspase-6 (CAS6_GALLUS; NP_990057; $aa_{49–299}$), caspase-3 (CAS3_GALLUS; NP_990056; $aa_{45–282}$), caspase-2 (CAS2_GALLUS; Q98943; $aa_{162–417}$), and caspase-1 (CAS1_GALLUS; NP_990255; $aa_{33–280}$); *S. domuncula* caspase–like protein (CASL_SUBDO); *D. melanogaster* caspase DCP-1; *Strongylocentrotus purpuratus* caspases: caspase-7 like (CAS7l_STROPU; XP_786037; $aa_{133–380}$) and caspase-6 like (CAS6l_STROPU; XP_789185; $aa_{73–325}$); *Caenorhabditis elegans* caspase CED-3 (CED3_CAEL; AAG42045; $aa_{235–495}$); metacaspase of *Schizosaccharomyces pombe* (METAC_SCHIPO; AAG38593; $aa_{130–415}$), and the peptidase C14 containing the caspase catalytic subunit p20 of *Nitrobacter* sp. (PC14_NITROB; ZP_01047279; $aa_{29–241}$), used as an outgroup.

Furthermore, several proteases that are more closely related to caspases than to other proteases of this class were identified in plants, fungi, and bacteria. They were termed meta- and paracaspases (Uren et al. 2000). Possibly they are also involved in cell death; however, their function remains to be elucidated.

Caspases can be grouped according to their prodomain structure into 2 broad classes (Salvesen and Dixit 1997; Thornberry et al. 1997). Initiator or apical caspases carry a large prodomain that comprises 1 of 2 protein–protein interaction domains, a death effector domain or a caspase recruitment domain. In contrast, effector or basal caspases

either lack or carry only a short prodomain. Because CASL features an uncommonly large COOH-terminal region and its prodomain consists of not more than 16 aa, for phylogenetic analyses only the large and small subunit–bearing CASc domain was considered to be of informative value. Thus, poriferan CASc was aligned with the corresponding domains of its closest relatives, including humans, chicken, *Xenopus laevis*, *S. purpuratus*, *D. melanogaster*, and *C. elegans* caspases as well as a metacaspase of *Schizosaccharomyces pombe*. The alignment revealed highest aa sequence homology to vertebrate caspase-7, sharing 21% identical and 37% similar aa with the human protein, 21%/35% with the *Xenopus* molecule, and 20%/35% with that of chicken. The homology to other caspases was slightly less, for example, chicken caspase-1 (13%/29%) and human caspase-12 (13%/30%), or considerably lower in case of the yeast metacaspase (8%/20%). A phylogenetic tree, based on this alignment, was rooted with the distantly related *Nitrobacter* Cys protease C14 containing the caspase catalytic subunit p20 (fig. 3*B*). The resulting tree revealed 6 clusters, comprising caspase-3 and -7 (1), caspase-6 and DCP-1 (2), caspase-8 and -10 (3), caspase-9 (4), caspase-2 and CED-3 (5), and a sixth cluster with a greater diversity, consisting of caspase-1, -4, -5, and -12 and the *D. rerio* caspase-2. No resolution as to the positioning of the yeast metacaspase could be obtained, likely due to the putative mitochondrial origin of metacaspases (Koonin and Aravind 2002). However, the positioning of the poriferan molecule CASL at the origin of the clusters reflects the ancient character of this protease, strongly supporting the monophyly of classic caspases.

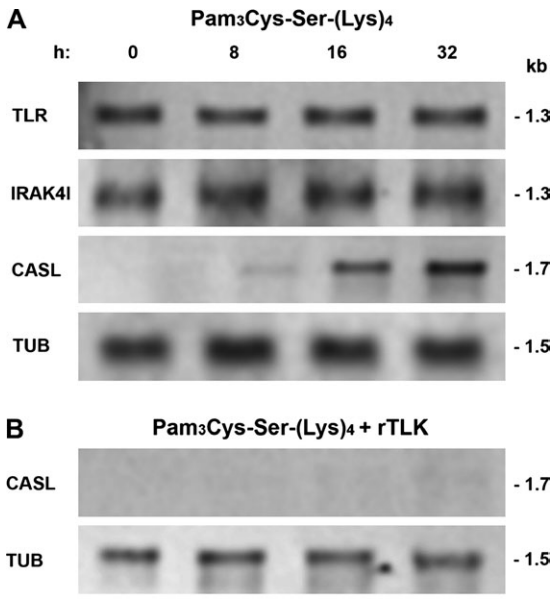


FIG. 4.—$Pam_3Cys\text{-}Ser\text{-}(Lys)_4$–induced gene expression in *S. domuncula*. (*A*) Following incubation of sponge tissue with the synthetic LP $Pam_3Cys\text{-}Ser\text{-}(Lys)_4$ for the indicated time, RNA was isolated, size separated (equal amounts of RNA were loaded), and blotted. The blots were probed for transcripts of poriferan TLR, IRAK-4l protein, CASL, and TUB. The latter one was used as an internal control. (*B*) $Pam_3Cys\text{-}Ser\text{-}(Lys)_4$ was pretreated with rTLR before it was applied to sponge tissue. After incubation of sponge tissue, RNA was isolated and again submitted to northern blot analyses.

## Gene Expression in Response to $Pam_3Cys\text{-}Ser\text{-}(Lys)_4$ Treatment

LPs are found abundantly in both gram-negative and gram-positive bacteria. They represent an important class of PAMPs and are known to induce a broad spectrum of host-defense mechanisms. In particular, the functional association of TLR-1 or TLR-6 with TLR-2 in response to diacyl and triacyl lipopeptides stimulates antimicrobial pathways (Brightbill et al. 1999; Ozinsky et al. 2000; Buwitt-Beckmann et al. 2005). (S)-[2,3-Bis(palmitoyloxy)-(2-RS)-propyl]-N-palmitoyl-(R)-Cys-(S)-Ser-(S)-$Lys_4$-OH·3HCl ($Pam_3Cys\text{-}Ser\text{-}(Lys)_4$) represents a synthetic (thus free from contaminating bacterial products) triacylated LP that is routinely used as an analog of bacterial LPs (e.g., Vasselon et al. 2004). Its direct binding to TLRs induces TLR heterodimerization and mimics the immunomodulatory effects of bacterial LP. Thus, after binding to TLRs, an active signaling complex is formed, including the adapter MyD88 and IRAK proteins, resulting in the production of antimicrobial compounds through the activation of transcription factors (Takeuchi et al. 2001, 2002; Buwitt-Beckmann et al. 2005).

Bacterial LPs and several other PAMPs have also been shown to trigger apoptosis through TLR-mediated signaling. This pathway probably bifurcates at the level of TLR-binding adapters, either via MyD88 and subsequent activation of the caspase cascade or via TRIF and subsequent stimulation of the intrinsic pathway (Aliprantis et al. 1999, 2000; Hsu et al. 2004), consequently resulting in an activation of the caspase cascade. Furthermore, bacterial LPs mediate activation of NF-κB. This transcription factor has also been implicated in the expression of both pro- and antiapoptotic genes (Baichwal and Baeuerle 1997; Wang et al. 1998), complementing the activation of pro- and antiapoptotic proteins on the transcriptional level.

In order to examine the effect of LPs on the expression of these proteins that are also putatively involved in poriferan antimicrobial mechanisms and because the poriferan TLR revealed closest sequence homology to the vertebrate TLR-1 and TLR-6, sponge tissue was incubated with $Pam_3Cys\text{-}Ser\text{-}(Lys)_4$ for 8 h, 16 h, and 32 h. After RNA isolation, electrophoresis, and blotting, the respective transcripts were identified by means of labeled probes, detecting the poriferan TLR, IRAK-4l protein, caspase-like protease, or TUB (the expression of this housekeeping gene was used as an internal control). The blotting experiments revealed a relatively high level of expression of TLR and IRAK-4l in the control tissue. Regardless of a $Pam_3Cys\text{-}Ser\text{-}(Lys)_4$ challenge (up to 32 h), the steady-state level of transcription of those genes remained unchanged. In contrast, transcripts of the CASL were not detectable in control tissue. However, after 8 h of $Pam_3Cys\text{-}Ser\text{-}(Lys)_4$ treatment, the CASL expression dramatically increased (fig. 4*A*).

In a second set of experiments, $Pam_3Cys\text{-}Ser\text{-}(Lys)_4$ was pretreated with recombinant TLR_SUBDO, the putative receptor of bacterial LPs. Only after this "blocking," the synthetic LPs were applied to sponge tissue for 8 h, 16 h, and 32 h. RNA of tissue thus treated was again subjected to northern blot analyses. The resulting blot revealed no $Pam_3Cys\text{-}Ser\text{-}(Lys)_4$–induced expression of CASL. The

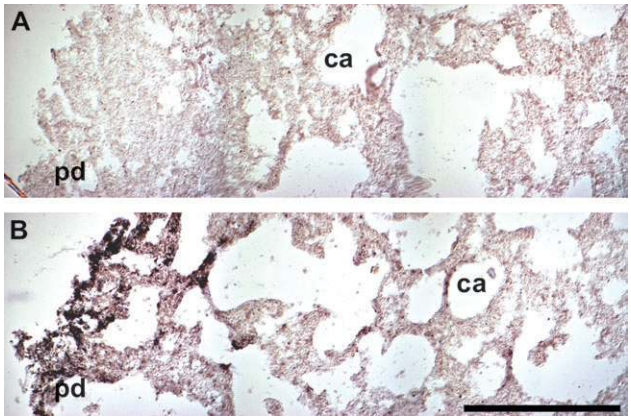


FIG. 5.—Localization of TLR-expressing cells within *S. domuncula* tissue: in situ analysis. Cryosections of sponge tissue were subjected to in situ hybridization analyses, using either labeled (*A*) TLR-sense probe (negative control) or (*B*) antisense probe. Hybridized probes were then detected through anti-DIG Fab fragments, conjugated to alkaline phosphatase, and subsequent NBT/BCIP treatment. The surface epithelial layer (pd; pinacoderm) and canals (ca) are marked. Scale bar, 1 mm.

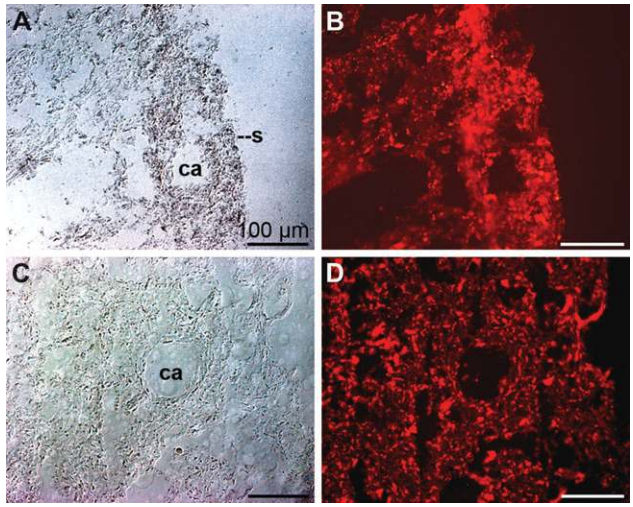


FIG. 6.—Localization of TLR-expressing cells within *S. domuncula* tissue: immunohistological analysis. Sections of sponge tissue were subjected to immunohistological analyses, using pAbs raised against TLR_SUBDO. Antigen/antibody complexes were identified with Cy3-conjugated secondary antibodies. Cells of the animal surface (s) are depicted in (*A*) Nomarsky and (*B*) immunofluorescence. Cells of the aquiferous canal (ca) system within the mesohyl are depicted in (*C*) Nomarsky and (*D*) immunofluorescence. Scale bars, 100 µm.

transcript level in treated samples was comparable to the steady-state level of expression of control samples (fig. 4*B*).

These results have several major implications. First, LPs are recognized by sponge cells and trigger the activation of transcription factors. Second, because a caspase is among those proteins whose expression is stimulated, apoptosis takes part in the antibacterial response. Third, LPs blocked with rTLR were not able to induce the transcription of CASL, consequently implying a potential role of TLR as a PRR of LPs. Fourth, TLR and IRAK-4l are constitutively expressed, thus allowing an immediate response to microbial threats, which is an imperative prerequisite of innate immunity.

These results taken together lend further proof to the concept that induction of apoptosis by TLRs is an evolutionarily conserved mechanism for innate immune defense. The relevance of TLR-mediated apoptosis, however, remains elusive, though the TLR-induced death of immune effector cells could control the duration of acute response to microbial assaults (Aliprantis et al. 2000).

### Localization of TLR-Expressing Cells within Sponge Tissue

Toll-like receptors are transmembrane proteins expressed in cells that are exposed to the environment. Some TLRs are located on the cell surface, whereas others remain sequestered in intracellular compartments (Akira et al. 2006). According to the sequence analyses, *S. domuncula* TLR displays the prerequisites for recognition of microbial invaders and subsequent innate immune response: an amino-terminal ectodomain–containing 4 leucine–bearing repeats, a transmembrane region (of 23 hydrophobic aa), and a COOH-terminal intracellular TIR domain. To further support the assumption that TLR_SUBDO represents a PRR and thus is part of the frontline, antimicrobial defense of sponges, in situ hybridization analyses were performed. For this purpose, sponge tissue cryosections were incubated with labeled sense or antisense probes of TLR. Hybridized probes were then detected via successive treatment with anti-DIG-AP antibodies and substrate. Although the sense probe did not produce any signal (fig. 5*A*), the antisense probe abundantly detected transcripts found in the surface cell layer of the pinacoderm and to a lower degree also in cells lining the aquiferous canal system within the mesohyl, the internal part of the sponge (fig. 5*B*).

In a parallel set of experiments, tissue sections were treated with pAbs raised against recombinant TLR_SUBDO. The resulting immunocomplexes were then detected with Cy3-conjugated secondary antibodies. These immunohistological analyses revealed again a TLR expression especially favoring the cells of the animal surface (fig. 6*A* and *B*) and the canal system (fig. 6*C* and *D*).

Thus, TLR is primarily expressed at the interface with the environment and meets another prerequisite of TLRs.

## Conclusion

It was Metchnikoff (1892) who first demonstrated the existence of innate immunity in sponges, primarily based on phagocytosis by sponge archaeocytes. With the introduction of molecular tools 100 years later, molecular biological and cell biological support for the presence of this immune system came from studies with the demosponges *S. domuncula* and *Geodia cydonium*. The studies clearly revealed that these animals, the closest relatives to the common ancestral phylum Urmetazoa (Müller 2001), are provided with key molecules involved in immune signaling pathways (see Introduction). Interestingly, only in some protostomian taxa, for example, *D. melanogaster*, the TLR-dependent control of innate immunity could be demonstrated. In contrast, the only *C. elegans* toll receptor homologue known so far does not appear to play such a role (Pujol et al. 2001). Thus, the results summarized in this

study, which demonstrated that a TLR-mediated antimicrobial defense in sponges exists, came unexpected. This is even more remarkable because—until now—also in the diploblastic Cnidaria a similar TLR has not been described.

In the present work, it is demonstrated that a poriferan TLR-like molecule (TLR_SUBDO), particularly localized in cells on the surface of the animals and in cells lining the aquiferous canal system, mediates LP-stimulated signal pathways, in which the IRAK-4l protein (IRAK4l_SUBDO) is potentially implicated. The constitutive expression of both proteins ensures an immediate response to bacterial challenge that ultimately leads to an increased expression of the caspase-like molecule CASL_SUBDO and subsequent initiation of the caspase-dependent apoptotic machinery. Competition experiments between the soluble recombinant sponge TLR and a synthetic lipopeptide further support the conclusion that this receptor is indeed involved in the innate immune defense of sponges.

TIR domain proteins and caspase-like proteins have been found in plants. Thus, the finding that the synthetic lipopeptide $Pam_3Cys\text{-}Ser\text{-}(Lys)_4$ elicits caspase induction via TLR (and potentially IRAK-4) in the poriferan system supports the suggestion that the TLR-dependent innate immunity–signaling pathway in Metazoa is the consequence of a convergent evolution of an analogous recognition system in plants (Ausubel 2005).

The poriferan TLR, IRAK-4l, and caspase sequences generally display the protein family–specific characteristics of higher Metazoa. Nevertheless, there appears to be several sponge-specific alterations and unusual variations of otherwise conserved patterns and motifs, probably relating to poriferan modifications of the "classic" innate immune response pathways.

Having gathered these data, future studies must reveal if the toll-like receptor, described here for the sponge *S. domuncula*, is the only existing poriferan member of the TLR family. However, considering the fact that sponges are exposed to a vast variety of potentially pathogenic microorganisms, it might be safe to predict a whole array of poriferan TLRs.

To conclude, these data demonstrate that sponges have a receptor-mediated antibacterial defense system, closely linked to the apoptotic cell death–executing system. The concerted action of these mechanisms, in combination with the previously described LPS-induced signaling pathways and the defense systems against fungi and virus (for references: see Introduction), granted a successful survival of the poriferan taxon throughout metazoan evolution.

## Supplementary Material

The following cDNA sequences from *S. domuncula* that have been deposited (EMBL/GenBank) as TLR (*SDTLR*; accession number AM392428), IRAK-4l Protein *SDIRAK-4l* (AM392429), and the CASL *SDCASL* (AM392430) are available at *Molecular Biology and Evolution* online (http://www.mbe.oxfordjournals.org/).

## Acknowledgments

This work was supported by grants from the Deutsche Forschungsgemeinschaft (WI 2116/2-1) and the Bundesministerium für Bildung und Forschung, Germany (project: Center of Excellence; BIOTECmarin).

## Literature Cited

Akira S. 2003. Toll-like receptor signaling. J Biol Chem. 278:38105–38108.

Akira S, Uematsu S, Takeuchi O. 2006. Pathogen recognition and innate immunity. Cell. 124:783–801.

Aliprantis AO, Yang RB, Mark MR, Suggett S, Devaux B, Radolf JD, Klimpel GR, Godowski P, Zychlinsky A. 1999. Cell activation and apoptosis by bacterial lipoproteins through toll-like receptor-2. Science. 285:736–739.

Aliprantis AO, Yang RB, Weiss DS, Godowski P, Zychlinsky A. 2000. The apoptotic signaling pathway activated by toll-like receptor-2. EMBO J. 19:3325–3336.

Ausubel FM. 2005. Are innate immune signalling pathways in plants and animals conserved? Nat Immunol. 6:973–979.

Baichwal VR, Baeuerle PA. 1997. Activate NF-κB or die? Curr Biol. 7:R94–R96.

Bell JK, Mullen GED, Leifer CA, Mazzoni A, Davies DR, Segal DM. 2003. Leucine-rich repeats and pathogen recognition in toll-like receptors. Trends Immunol. 24:528–533.

Bergh O, Borsheim KY, Bratbak G, Heldal M. 1989. High abundance of viruses found in aquatic environments. Nature. 340:467–468.

Blumbach B, Pancer Z, Diehl-Seifert B, Steffen R, Münkner J, Müller IM, Müller WEG. 1998. The putative sponge aggregation receptor: isolation and characterization of a molecule composed of scavenger receptor cysteine-rich domains and short consensus repeats. J Cell Sci. 111:2635–2644.

Böhm M, Hentschel U, Friedrich A, Fieseler L, Steffen R, Gamulin V, Müller IM, Müller WEG. 2001. Molecular response of the sponge *Suberites domuncula* to bacterial infection. Mar Biol. 139:1037–1045.

Böhm M, Müller IM, Müller WEG, Gamulin V. 2000. The mitogen-activated protein kinase p38 pathway is conserved in metazoans: cloning and activation of p38 of the SAPK2 subfamily from the sponge *Suberites domuncula*. Biol Cell. 29:95–104.

Brightbill HD, Libraty DH, Krutzik SR, et al. (14 co-authors). 1999. Host defense mechanisms triggered by microbial lipoproteins through toll-like receptors. Science. 285:732–736.

Buwitt-Beckmann U, Heine H, Wiesmuller KH, Jung G, Brock R, Akira S, Ulmer AJ. 2005. Toll-like receptor 6-independent signaling by diacylated lipopeptides. Eur J Immunol. 35:282–289.

Coligan JE, Dunn BM, Ploegh HL, Speicher DW, Wingfield PT. 2000. Current protocols in protein science. New York: John Wiley & Sons, Inc. p. 2.0.1–2.8.17.

Dayhoff MO, Schwartz RM, Orcutt BC. 1978. In: Dayhoff MO, editor. Atlas of protein sequence and structure. Washington (DC): National Biomedical Research Foundation. p. 345–352.

Faulkner DJ. 2002. Marine natural products. Nat Prod Rep. 19: 1–48.

Felsenstein J. 1993. PHYLIP—phylogeny inference package. Cladistics. 5:164–166.

Finn RD, Mistry J, Schuster-Böckler B, et al. (13 co-authors). 2006. Pfam: clans, web tools and services. Nucleic Acids Res. 34:D247–D251.

Francois S, El Benna J, Dang PM, Pedruzzi E, Gougerot-Pocidalo MA, Elbim C. 2005. Inhibition of neutrophil apoptosis by TLR agonists in whole blood: involvement of the phosphoinositide 3-kinase/Akt and NF-kappaB signaling pathways, leading to increased levels of Mcl-1, A1, and phosphorylated Bad. J Immunol. 174:3633–3642.

Grebenjuk VA, Kuusksalu A, Kelve M, Schütze J, Schröder HC, Müller WEG. 2002. Induction of (2′-5′)oligoadenylate synthetase in the marine sponges *Suberites domuncula* and *Geodia cydonium* by the bacterial endotoxin lipopolysaccharide. Eur J Biochem. 269:1382–1392.

Harlow E, Lane D. 1988. Antibodies: a laboratory manual. Cold Spring Harbor (NY): Cold Spring Harbor Laboratory.

Hashimoto C, Hudson KL, Anderson KV. 1988. The toll gene of *Drosophila*, required for dorsal-ventral embryonic polarity, appears to encode a transmembrane protein. Cell. 52:269–279.

Hochuli E, Döbeli H, Schacher A. 1987. New metal chelate adsorbent selective for proteins and peptides containing neighbouring histidine residues. J Chromatogr. 411:177–184.

Hsu LC, Park JM, Zhang K, Luo JL, Maeda S, Kaufman RJ, Eckmann L, Guiney DG, Karin M. 2004. The protein kinase PKR is required for macrophage apoptosis after activation of toll-like receptor 4. Nature. 428:341–345.

Jebanathirajah J, Peri S, Pandey A. 2002. Toll and interleukin-1 receptor (TIR) domain-containing proteins in plants: a genomic perspective. Trends Plant Sci. 7:388–391.

Koonin EV, Aravind L. 2002. Origin and evolution of eukaryotic apoptosis: the bacterial connection. Cell Death Differ. 9:394–404.

Kruse M, Müller IM, Müller WEG. 1997. Early evolution of metazoan serine/threonine- and tyrosine kinases: identification of selected kinases in marine sponges. Mol Biol Evol. 14:1326–1334.

Kyte J, Doolittle RF. 1982. A simple method for displaying the hydropathic character of a protein. J Mol Biol. 157:105–132.

Laemmli UK. 1970. Cleavage of structural proteins during the assembly of the head of bacteriophage T4. Nature. 227:680–685.

Laukner G. 1980. Diseases of Porifera. In: Kinne O, editor. Diseases of marine animals. Chichester (United Kingdom): Wiley.

Lemaitre B, Nicholas E, Michaut L, Reichhart JM, Hoffmann JA. 1996. The dorsoventral regulatory gene cassette spatzle/Toll/cactus controls the potent antifungal response in *Drosophila* adults. Cell. 86:973–983.

Letunic I, Copley RR, Pils B, Pinkert S, Schultz J, Bork P. 2006. SMART 5: domains in the context of genomes and networks. Nucleic Acids Res. 34:D257–D260.

Li S, Strelow A, Fontana EJ, Wesche H. 2002. IRAK-4: a novel member of the IRAK family with the properties of an IRAK-kinase. Proc Natl Acad Sci USA. 99:5567–5572.

Lowry OH, Rosebrough NJ, Farr AL, Randall RJ. 1951. Protein measurement with the Folin phenol reagent. J Biol Chem. 193:265–275.

Martin M, Bol GF, Eriksson A, Resch K, Brigelius-Flohe R. 1994. Interleukin-1-induced activation of a protein kinase coprecipitating with the type I interleukin-1 receptor in T cells. Eur J Immunol. 24:1566–1571.

Medzhitov R, Janeway C. 2000. The toll receptor family and microbial recognition. Trends Microbiol. 8:452–456.

Metchnikoff E. 1892. Leçons sur la pathologie comparée de l'inflammation. Paris: G. Masson.

Müller WEG. 2001. How was metazoan threshold crossed: the hypothetical Urmetazoa. Comp Biochem Physiol A. 129:433–460.

Nicholas KB, Nicholas HB Jr. 1997. GeneDoc: a tool for editing and annotating multiple sequence alignments. Version 2.6.002 [Internet]. Distributed by the authors [cited 2007 Jan 22]. Available from: http://www.psc.edu/biomed/genedoc/.

Ozinsky A, Underhill DM, Fontenot JD, Hajjar AM, Smith KD, Wilson CB, Schroeder L, Aderem A. 2000. The repertoire for pattern recognition of pathogens by the innate immune system is defined by cooperation between toll-like receptors. Proc Natl Acad Sci USA. 97:13766–13771.

Pahler S, Blumbach B, Müller I, Müller WEG. 1998. A putative multiadhesive basal lamina protein from the marine sponge *Geodia cydonium*: cloning of the cDNA encoding a fibronectin-, an SRCR- as well as a complement control protein module. J Exp Zool. 282:332–343.

Perović S, Schröder HC, Sudek S, Grebenjuk VA, Batel R, Štifanić M, Müller IM, Müller WEG. 2003. Expression of one sponge *Iroquois* homeobox gene in primmorphs from *Suberites domuncula* during canal formation. Evol Dev. 5:240–250.

Perović-Ottstadt S, Adell T, Proksch P, Wiens M, Korzhev M, Gamulin V, Müller IM, Müller WEG. 2004. A (1→3)-*β*-D-glucan recognition protein from the sponge *Suberites domuncula*: mediated activation of fibrinogen-like protein and epidermal growth factor gene expression. Eur J Biochem. 271:1924–1937.

Polak JM, McGee JD. 1998. In situ hybridization. Oxford: Oxford University Press.

Proksch P. 1994. Defensive roles for secondary metabolites from marine sponges and sponge-feeding nudibranchs. Toxicon. 32:639–655.

Pujol N, Link EM, Liu LX, Kurz CL, Alloing G, Tan MW, Ray KP, Solari R, Johnson CD, Ewbank JJ. 2001. A reverse genetic analysis of components of the toll signaling pathway in *Caenorhabditis elegans*. Curr Biol. 11:809–821.

Saitou N, Nei M. 1987. The neighbor-joining method: a new method for reconstructing phylogenetic trees. Mol Biol Evol. 4:406–425.

Salvesen GS, Dixit VM. 1997. Caspases: intracellular signaling by proteolysis. Cell. 91:443–446.

Sarma AS, Daum T, Müller WEG. 1993. Secondary metabolites from marine sponges. Verlag (Berlin): Akademie gemeinnütziger Wissenschaften zu Erfurt, Ullstein-Mosby.

Srinivasula SM, Fernandes-Alnemri T, Zangrilli J, Robertson N, Armstrong RC, Wang L, Trapani JA, Tomaselli KJ, Litwack G, Alnemri ES. 1996. The Ced-3/interleukin 1beta converting enzyme-like homolog Mch6 and the lamin-cleaving enzyme Mch2 alpha are substrates for the apoptotic mediator CPP32. J Biol Chem. 271:27099–27106.

Steward GF, Smith DC, Azam F. 1996. Abundance and production of bacteria and viruses in the Bering and Chukchi Seas. Mar Ecol Prog Ser. 131:287–300.

Takahashi A, Earnshaw WC. 1996. ICE-related proteases in apoptosis. Curr Opin Genet Dev. 6:50–55.

Takeda K. 2005. Evolution and integration of innate immune recognition systems: the toll-like receptors. J Endotoxin Res. 11:51–55.

Takeuchi O, Kawai T, Muhlradt PF, Morr M, Radolf JD, Zychlinsky A, Takeda K, Akira S. 2001. Discrimination of bacterial lipoproteins by Toll-like receptor 6. Int Immunol. 13:933–940.

Takeuchi O, Sato S, Horiuchi T, Hoshino K, Takeda K, Dong Z, Modlin RL, Akira S. 2002. Cutting edge: role of Toll-like receptor 1 in mediating immune response to microbial lipoproteins. J Immunol. 169:10–14.

Talanian RV, Quinlan C, Trautz S, Hackett MC, Mankovitch JA, Banach D, Ghayur T, Brady KD, Wong WW. 1997. Substrate specificities of caspase family proteases. J Biol Chem. 272:9677–9682.

Thakur NL, Perović-Ottstadt S, Batel R, Korzhev M, Diehl-Seifert B, Müller IM, Müller WEG. 2005. Innate immune defense of the sponge *Suberites domuncula* against gram-positive bacteria: induction of lysozyme and AdaPTin. Mar Biol. 146:271–282.

Thompson JD, Higgins DG, Gibson TJ. 1994. CLUSTAL W: improving the sensitivity of progressive multiple sequence alignment through sequence weighting, position-specific gap penalties and weight matrix choice. Nucleic Acids Res. 22:4673–4680.

Thornberry NA, Lazebnik Y. 1998. Caspases: enemies within. Science. 281:1312–1316.

Thornberry NA, Rano TA, Peterson EP, et al. (12 co-authors). 1997. A combinatorial approach defines specificities of members of the caspase family and granzyme B. Functional relationships established for key mediators of apoptosis. J Biol Chem. 272:17907–17911.

Underhill DM, Ozinsky A. 2002. Toll-like receptors: key mediators of microbial detection. Curr Opin Immunol. 14:103–110.

Uren AG, O'Rourke K, Aravind L, Pisabarro MT, Seshagiri S, Koonin EV, Dixit VM. 2000. Identification of paracaspases and metacaspases: two ancient families of caspase-related proteins, one of which plays a central role in MALT lymphoma. Mol Cell. 6:961–967.

Vacelet J, Vacelet E, Gaino E, Gallissian MF. 1994. Bacterial attack of spongin skeleton during the 1986-1990 Mediterranean sponge disease. In: Van Soest RWM, Van Kempen TMG, Braekman JC. editors. Sponges in time and space. Rotterdam (The Netherlands): Balkema. p. 355–362.

Vasselon T, Detmers PA, Charron D, Haziot A. 2004. TLR2 recognizes a bacterial lipopeptide through direct binding. J Immunol. 173:7401–7405.

Wang CY, Mayo MW, Korneluk RG, Goeddel DV, Baldwin AS Jr. 1998. NF-κB antiapoptosis: induction of TRAF1 and TRAF2 and c-IAP1 and c-IAP2 to suppress caspase-8 activation. Science. 281:1680–1683.

Wesche H, Gao X, Li X, Kirschning CJ, Stark GR, Cao Z. 1999. IRAK-M is a novel member of the pelle/interleukin-1 receptor associated kinase (IRAK) family. J Biol Chem. 274:19403–19410.

Wiens M, Korzhev M, Krasko A, Thakur NL, Perović-Ottstadt S, Breter HJ, Ushijima H, Diehl-Seifert B, Müller IM, Müller WEG. 2005. Innate immune defense of the sponge *Suberites domuncula* against bacteria involves a MyD88-dependent signaling pathway. Induction of a perforin-like molecule. J Biol Chem. 280:27949–27959.

Wiens M, Kuusksalu A, Kelve M, Müller WEG. 1999. Origin of the interferon-inducible (2′-5′)oligoadenylate synthetases: cloning of the (2′-5′)oligoadenylate synthetase from the marine sponge *Geodia cydonium*. FEBS Lett. 462:12–18.

Wiens M, Müller WEG. 2006. Cell death in Porifera: molecular players in the game of apoptotic cell death in living fossils. Can J Zool. 84:307–321.

Wilson HV. 1907. On some phenomena of coalescence and regeneration in sponges. J Exp Zool. 5:245–258.

Wimmer W, Blumbach B, Diehl-Seifert B, Koziol C, Batel R, Steffen R, Müller IM, Müller WEG. 1999. Increased expression of integrin and receptor tyrosine kinase genes during autograft fusion in the sponge *Geodia cydonium*. Cell Adhes Commun. 260:156–165.

Yuan J, Shaham S, Ledoux S, Ellis HM, Horvitz HR. 1993. The *C. elegans* cell death gene ced-3 encodes a protein similar to mammalian interleukin-1 beta-converting enzyme. Cell. 75:641–652.

Billie Swalla, Associate Editor

Accepted December 18, 2006